4 × 20 Gbit/s mode division multiplexing over free space using vector modes and a *q*-plate mode (de)multiplexer

Giovanni Milione,[1,2,3,4,*] Martin P. J. Lavery,[5] Hao Huang,[6] Yongxiong Ren,[6] Guodong Xie,[6] Thien An Nguyen,[1,2] Ebrahim Karimi,[7] Lorenzo Marrucci,[4,8] Daniel A. Nolan,[4,9] Robert R. Alfano,[1,2,3,4] and Alan E. Willner[6]

[1]*Institute for Ultrafast Spectroscopy and Lasers, New York 10031, USA*

[2]*Physics Department, City College of the City University of New York, New York 10031, USA*

[3]*Physics Department, Graduate Center of the City University of New York, New York 10016, USA*

[4]*New York State Center for Complex Light, New York 10031, USA*

[5]*School of Engineering, University of Glasgow, Glasgow G12 8QQ, Scotland, UK*

[6]*Department of Electrical Engineering, University of Southern California, Los Angeles, California 90089, USA*

[7]*Department of Physics, University of Ottawa, Ottawa, Ontario K1N 6N5, Canada*

[8]*Dipartimento di Fisica, Universita di Napoli Federico II, Complesso Universitario di Monte Sant'Angelo, Napoli, Italy*

[9]*Corning Incorporated, Sullivan Park, Corning, New York 14831, USA*

*Corresponding author: giomilione@gmail.com

Vector modes are spatial modes that have spatially inhomogeneous states of polarization, such as, radial and azimuthal polarization. In this work, the spatially inhomogeneous states of polarization of vector modes are used to increase the transmission data rate of free-space optical communication via mode division multiplexing. A mode (de)multiplexer for vector modes based on a liquid crystal *q*-plate is introduced. As a proof of principle, four vector modes each carrying a 20-Gbit/s quadrature phase shift keying signal (aggregate 80 Gbit/s) on a single wavelength channel ($\lambda \sim 1550$ nm) were transmitted ~1 m over the lab table with < -16.4 dB mode crosstalk. Bit error rates for all vector modes were measured at the 7% forward error correction threshold with power penalties <3.41 dB.   © 2015 Optical Society of America

OCIS codes: (010.1330) Atmospheric turbulence; (060.2605) Free-space optical communication; (060.4510) Optical communications; (260.6042) Singular optics; (050.4865) Optical vortices; (060.4230) Multiplexing.

http://dx.doi.org/10.1364/OL.40.001980

Mode division multiplexing (MDM) is the method of optical communication where spatial modes are used as information channels carrying independent data streams. Potentially, MDM can be used to increase the transmission data rate of optical communication in an amount proportional to the number of modes used. MDM has been used in optical fiber communication [1]. Potentially, MDM can also be used in free-space optical communication (FSO) [2]. Spatial modes can be represented by many bases [3]. In principle, any basis can be used for MDM. For example, what is sometimes referred to as the basis of orbital angular momentum (OAM) modes has been used in FSO [4]. There is also a basis referred to as the basis of vector modes (vector beams). Vector modes have spatially inhomogeneous states of polarization, such as, radial and azimuthal polarization. The spatially inhomogeneous states of polarization of vector modes can be used for many applications, including optical trapping and nanoscale imaging [5].

In this work, the spatially inhomogeneous states of polarization of vector modes are used to increase the transmission data rate of FSO via MDM. A mode (de)multiplexer for vector modes based on a liquid crystal *q*-plate is introduced. As a proof of principle, four vector modes each carrying a 20-Gbit/s quadrature phase shift keying signal (aggregate 80 Gbit/s) on a single wavelength channel ($\lambda \sim 1550$ nm) were transmitted ~1 m over the lab table, with < -16.4 dB mode crosstalk. Bit error rates for all vector modes were measured at the 7% forward error correction threshold with power penalties <3.41 dB.

A vector mode is defined here as a solution to the wave equation whose electric field is given by $\mathbf{E}(r, \phi) = f(r)\mathbf{V}_{\ell,\gamma}(\phi)$ [5]. (r, ϕ) are cylindrical coordinates, and $f(r)$ is a solution to the radial part of the wave equation, e.g., Bessel–Guassian functions [6]. $\mathbf{V}_{\ell,\gamma}(\phi)$ is a Jones vector that describes the spatially inhomogeneous state of polarization of a vector mode and is given by $\mathbf{V}_{\ell,\gamma}(\phi) = (\cos(\ell\phi + \gamma) \sin(\ell\phi + \gamma))^T$ ($\ell = 0, \pm 1, \pm 2, \ldots;$ $\gamma = 0, \pi/2$) [7]. For example, $\mathbf{V}_{+1,0}$ and $\mathbf{V}_{+1,\pi/2}$ are radial [Fig. 1(a1)] and azimuthal [Fig. 1(a2)] polarization, respectively. Note, the number of vector modes that can be used for MDM is theoretically unbounded. There are other examples of light fields that have spatially inhomogeneous states of polarization, e.g., [8]. However, not all light fields are solutions to the wave equation. If a light field is to be used for MDM, it must be a solution to the wave equation, i.e., its spatially inhomogeneous state of polarization must not change as it propagates.

To use vector modes for MDM, a mode (de)multiplexer for vector modes is required. A mode (de)multiplexer (separates) combines N spatial modes at the (receiver) transmitter of an optical communication system. For example, a mode (de)multiplexer for OAM modes that has been demonstrated is based on passive beam (separation) combining [4], e.g., data streams from N single-mode optical fibers (SMFs) are transformed into N OAM modes via N spatial light modulators (SLMs), or vice versa, and are then (separated) combined via $N - 1$ beam splitters. There are many methods to generate vector modes, e.g., [9–11]. Here, a liquid crystal technology
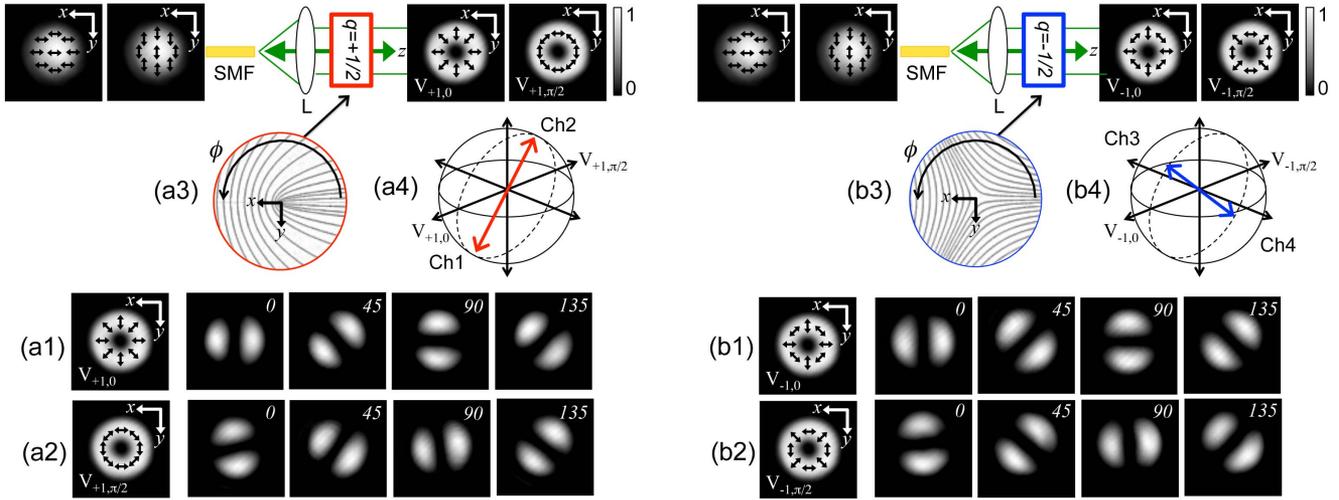
Fig. 1. Transformation of the state of polarization of the fundamental mode of a SMF into a linear combination of vector modes using a liquid crystal q-plate as described in the text: (a) $q = +1/2$ plate, (b) $q = -1/2$ plate.

referred to as a q-plate is used [12]. A q-plate comprises a thin layer of patterned liquid crystal molecules in-between two thin glass plates whose pattern is described by $q\phi$, where q is a half-integer. $q = +1/2$ and $q = -1/2$ plates are schematically shown in Figs. 1(a3) and 1(b3), respectively. Using a $q = +1/2$ or $q = -1/2$ plate, horizontal/vertical polarization of the fundamental mode of a SMF can be transformed into $V_{+1,0}(\phi)/V_{+1,\pi/2}(\phi)$ or $V_{-1,0}(\phi)/V_{-1,\pi/2}(\phi)$ vector modes, or vice versa, as schematically shown in Figs. 1(a) and 1(b), respectively.

Two $q = +1/2$ and $q = -1/2$ plates were fabricated [13]. Using the q-plates, a mode (de)multiplexer for vector modes based on passive beam (separation) combining was constructed as shown in Fig. 2. As a mode multiplexer, the fundamental modes of two SMFs at $\lambda \sim$ 1550 nm were collimated to beam waists of ~ 3 mm using appropriate lenses (L) and then made to propagate through the q-plates. Then, the light beams from each SMF were aligned co-linearly via a non-polarizing beam splitter (BS). A tunable voltage was applied over each q-plate using signal generators. The q-plates could be "turned on" and "turned off" by controlling the voltage [14]. Each q-plate was "turned on" (~ 1.2 Volts). Each q-plate has a ~ -1.16 dB transmission loss. $V_{+1,0}(\phi)/$ $V_{+1,\pi/2}(\phi)$ and $V_{-1,0}(\phi)/V_{-1,\pi/2}(\phi)$ vector modes as generated using the mode (de)multiplexer are shown in
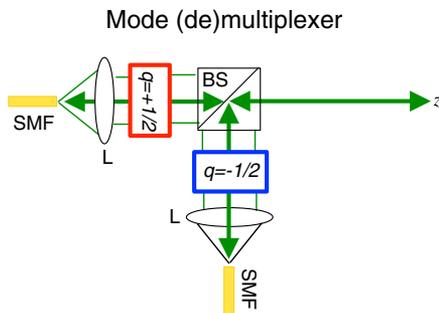

Mode (de)multiplexer

Fig. 2. Mode (de)multiplexer for vector modes based on passive beam (separation) combing as described in text. Green arrows indicates the light beam's direction of propagation.

Figs. 1(a1)/1(a2) and 1(b1)/1(b2), respectively. Also shown are the intensities of each vector mode as analyzed by a linear polarizer whose transmission axis is oriented at 0, 45, 90, and 135 degrees with respect to the lab table.

Using the mode (de)multiplexer, four vector modes, each carrying a 20-Gbit/s quadrature phase shift keyed (QPSK) signal (aggregate 80 Gbit/s) on a single wavelength channel ($\lambda \sim 1550$ nm) were transmitted as one light beam ~ 1 m over the lab table. Note, over this distance, there is negligible atmospheric turbulence and beam divergence. The experimental setup is shown in Fig. 2. At the transmitter, a 20-Gbit/s QPSK signal, being a pseudo-random-binary-bit-sequences of length $2^{15}-1$, was generated by modulating with an I-Q modulator the output of an external cavity laser (ECL) tuned to $\lambda \sim 1550$ nm. The signal was then amplified by a low-noise erbium-doped fiber amplifier (EDFA) and polarization division multiplexed (PDM) via its decorrelation in two SMFs whose states of polarization were mutually orthogonal, e.g., horizontal/vertical. The resultant PDM-QPSK signal was mode multiplexed via its decorrelation in two more SMFs that were then connected to the SMFs of the mode (de)multiplexer.

Due to twists and bends in the SMFs, the channels of each PDM-QPSK signal were not necessarily horizontal and vertical polarization. While they can be aligned using a polarization paddle controller (Pol-Con), in general, each channel is a linear combination of horizontal and vertical polarization. Effectively, the PDM-QPSK signals were transformed by the q-plates into a linear combination of vector modes as represented by two arbitrary antipodal points on a higher order Poincaré sphere [15,16]. The channels originating from the $q = +1/2$ and $q = -1/2$ plates are labelled Ch1/Ch2 [Fig. 1(a4)] and Ch3/Ch4 [Fig. 1(b4)]. Their intensities are shown in Figs. 3(a) and 3(b), respectively.

After transmission over the lab table, the receiver was as follows. First, the channels were mode demultiplexed into the two SMFs of another mode (de)multiplexer. The intensities of Ch1/Ch2 and Ch3/Ch4 at the SMF corresponding to the $q = +1/2$ q-plate are shown in Figs. 3(c) and 3(d), respectively. As can be seen, Ch1/Ch2
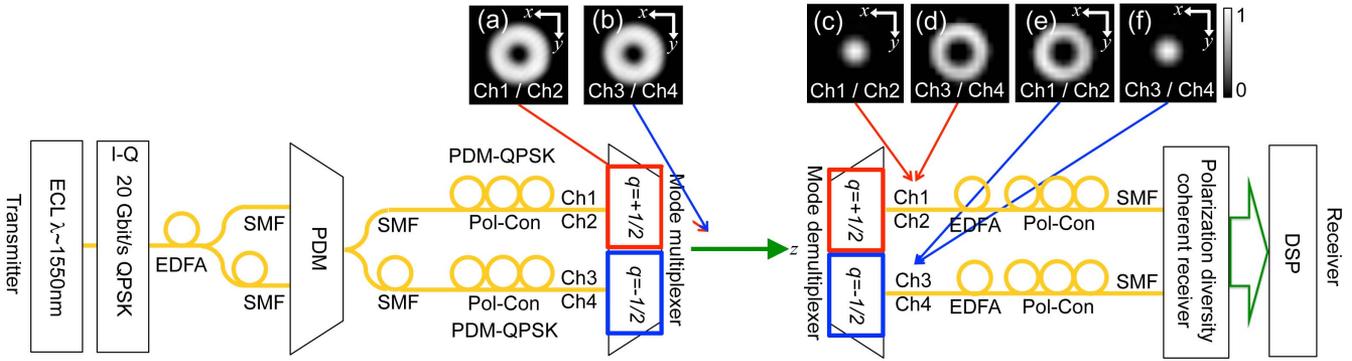
Fig. 3. Experimental setup for MDM using vector modes as described in the text.

were transformed back into the fundamental mode of a SMF, i.e, a PDM-QPSK signal, and were coupled to the SMF. However, Ch3/Ch4 were transformed into higher order vector modes and were not coupled to the SMF. The opposite is true for the $q = -1/2$ plate. The intensities of Ch1/Ch2 and Ch3/Ch4 at the SMF corresponding to the $q = -1/2$ plate are shown in Figs. 3(e) and 3(f), respectively. The resulting PDM-QPSK signals were then amplified by an EDFA and aligned via a Pol-Con to a polarization diversity coherent receiver where they were then polarization demultiplexed and coherently detected via intradyne detection. Using four balanced detectors, the analog QPSK signals were converted to digital signals and captured at 40 GSample/s ($\Delta 20$ GHz) via four digital oscilloscopes for offline digital signal processing (DSP). The captured constellations of the QPSK signals for all channels are shown in Fig. 4(a). As can be seen, the constellations for each channel differ slightly. This is attributed to mode-dependent loss (MDL). MDL is most likely due to imperfectly generated vector modes at the multiplexer, i.e., power is generated in vector modes (e.g., higher-order vector modes) other than the ones intended. Also, MDL is most likely attributed to misalignment of the transmitted light beam with respect to the q-plates of the demultiplexer, which results in a transfer of power to vector modes (e.g., higher-order vector modes) that are not detected by the q-plates.

Mode crosstalk (MC) for each channel was measured at the mode demultiplexer by transmitting one channel at a time and then measuring the power received by each of all channels. MC is defined as the transfer of power (signals) between channels. A normalized MC "matrix" comprising the MC measurements is shown in Fig. 4(b). There is < -16.7 dB MC for any channel. The sources of MC most likely include misalignment of the lenses and mismatch of the numerical apertures with respect to the SMFs of the demultiplexer. Also, sources of MC are most likely similar to the sources of MDL discussed above.

For each channel and a "back to back" (B2B) channel, bit error rates (BER) were measured as a function of optical signal-to-noise ratio (OSNR) when all channels were simultaneously transmitted. The B2B channel is the original QPSK signal, transmitted and received, when the q-plates are turned off. BER versus OSNR curves are shown in Fig. 4(c). The performance of each channel was assessed via its power penalty (PP), i.e., the difference in

OSNR between each channel and the B2B channel at a 7% forward error correction (FEC) threshold (BER = 3.8×10^{-3}). The PPs for Ch1, Ch2, Ch3, and Ch4 were 0.44 dB, 3,40 dB, 1.46 dB, and 0.41 dB, respectively. All channels reached a BER at the 7% FEC threshold with a PP <3.41 dB. Differences in PPs are attributed to MC and MDL as discussed above.

In conclusion, the spatially inhomogeneous states of polarization of vector modes were used to increase the
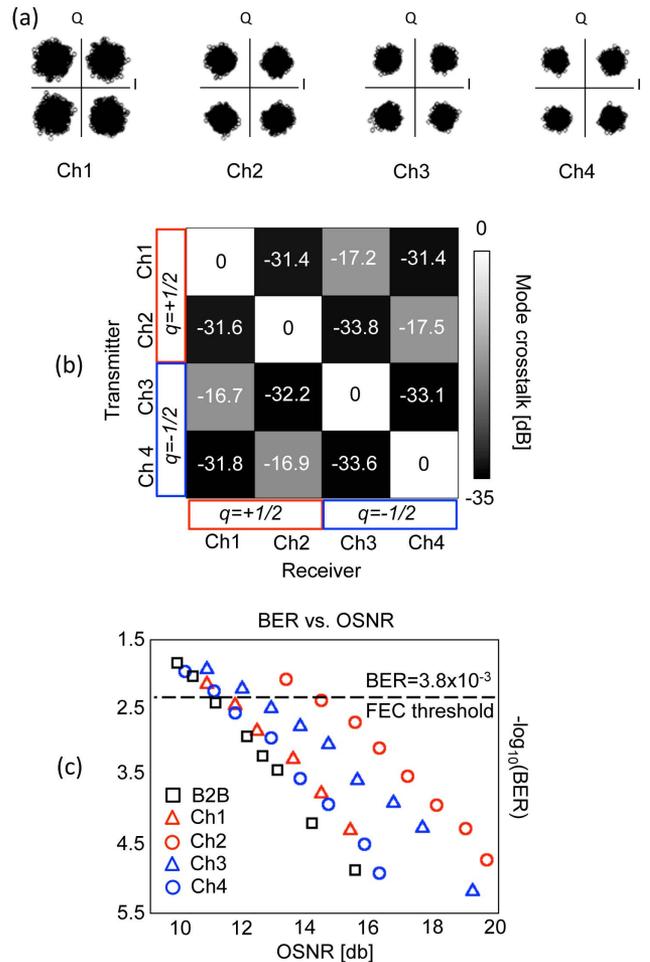

Fig. 4. (a) QPSK constellations for Ch1, Ch2, Ch3, and Ch4. (b) MC matrix for Ch1, Ch2, Ch3, and Ch4. (c) BER versus OSNR curves for Ch1, Ch2, Ch3, Ch4, and B2B.

transmission data rate of FSO via MDM. To the best of our knowledge, this is the first time vector modes have been used in MDM. A mode (de)multiplexer for vector modes based on a liquid crystal q-plate was introduced. As a proof of principle, four vector modes each carrying a 20-Gbit/s quadrature phase shift keying signal (aggregate 80 Gbit/s) on a single wavelength channel ($\lambda \sim 1550$ nm) were transmitted ~ 1 m over the lab table, with < -16.4 dB mode crosstalk. BERs for all vector modes were measured at the 7%FEC threshold with PPs <3.41 dB.

A major challenge for using MDM in FSO is atmospheric turbulence [17]. It has been conjectured upon propagation through atmospheric turbulence a vector mode will experience less scintillation as compared to, for example, an OAM mode [18]. The propagation of vector modes through atmospheric turbulence is the subject of future work. The radially dependent amplitudes of vector modes and OAM modes are expected to be comparable; it is anticipated that the divergence of vector modes as they propagate through atmospheric turbulence is comparable to that of OAM modes.

When using OAM modes for MDM, the deleterious effects of atmospheric turbulence can be compensated via wavefront measurements [19]. When using vector modes for MDM, comparable compensation of atmospheric turbulence or light scattering may be possible via the measurement of spatially inhomogeneous polarization [20,21]. Also, vector modes are the "true modes" of an optical fiber [3]. The use of the q-plate mode (de)multiplexer for optical fiber communication is the subject of current work [22,23].

References

1. D. J. Richardson, J. M. Fini, and L. E. Nelson, Nat. Photonics **7**, 354 (2013).
2. H. Willebrand and B. Ghuman, IEEE Spectr. **38**, 40 (2001).
3. R. J. Black and L. Gagnon, *Optical Waveguide Modes: Polarization, Coupling and Symmetry* (McGraw-Hill, 2009).
4. H. Huang, G. Xie, Y. Yan, N. Ahmed, Y. Ren, Y. Yue, D. Rogawski, M. J. Willner, B. I. Erkmen, K. M. Birnbaum, S. J. Dolinar, M. P. J. Lavery, and M. J. Padgett, Opt. Lett. **39**, 197 (2014).
5. Q. Zhan, Adv. Opt. Photonics **1**, 1 (2009).
6. G. Milione, A. Dudley, T. A. Nguyen, K. Chakraborty, E. Karimi, A. Forbes, and R. R. Alfano, J. Opt. **17**, 035617 (2015).
7. M. Stalder and M. Schadt, Opt. Lett. **21**, 1948 (1996).
8. G. M. Philip, V. Kumar, G. Milione, and N. K. Viswanathan, Opt. Lett. **37**, 2667 (2012).
9. H. I. Sztul, D. A. Nolan, G. Milione, X. Chen, J. Koh, and R. R. Alfano, Proc. SPIE **7227**, 722704 (2009).
10. G. Milione, H. I. Sztul, D. A. Nolan, J. Kim, M. Etienne, J. McCarthy, J. Wang, and R. R. Alfano, Proc. SPIE **7950**, 79500K (2011).
11. G. Milione, H. Sztul, D. Nolan, J. Kim, M. Etienne, J. McCarthy, J. Wang, and R. Alfano, "Cylindrical vector beam generation from a multi elliptical core optical fiber," in *CLEO:2011–Laser Applications to Photonic Applications*, OSA Technical Digest (CD) (Optical Society of America, 2011), paper CTuB2.
12. F. Cardano, E. Karimi, S. Slussarenko, L. Marrucci, C. de Lisio, and E. Santamato, Appl. Opt. **51**, C1 (2012).
13. S. Slussarenko, B. Piccirillo, V. Chigrinov, L. Marrucci, and E. Santamato, J. Opt. **15**, 025406 (2013).
14. Y. Rumala, G. Milione, T. Nguyen, S. Pratavieira, Z. Hossain, D. Nolan, S. Slussarenko, E. Karimi, L. Marrucci, and R. Alfano, Opt. Lett. **38**, 5083 (2013).
15. G. Milione, H. I. Sztul, D. A. Nolan, and R. R. Alfano, Phys. Rev. Lett. **107**, 053601 (2011).
16. G. Milione, S. E. Evans, D. A. Nolan, and R. R. Alfano, Phys. Rev. Lett. **108**, 190401 (2012).
17. M. J. Padgett, F. M. Miatto, M. P. J. Lavery, A. Zeilinger, and R. W. Boyd, New J. Phys. **17**, 023011 (2015).
18. W. Cheng, J. Haus, and Q. Zhan, Opt. Express **17**, 17829 (2009).
19. Y. Ren, G. Xie, H. Huang, N. Ahmed, Y. Yan, L. Li, C. Bao, M. Lavery, M. Tur, M. Neifeld, R. Boyd, J. Shapiro, and A. Willner, Optica **1**, 376 (2014).
20. A. Dudley, G. Milione, R. R. Alfano, and A. Forbes, Opt. Express **22**, 14031 (2014).
21. P. Shumyatsky, G. Milione, and R. R. Alfano, Opt. Commun. **321**, 116 (2014).
22. C. N. Alexeyev, A. N. Alexeyev, B. P. Lapin, G. Milione, and M. A. Yavorsky, Phys. Rev. A **88**, 063814 (2013).
23. G. Milione, D. A. Nolan, and R. R. Alfano, J. Opt. Soc. Am. B **32**, 143 (2015).